CHEMICAL ENGINEERING TRANSACTIONS
VOL. 32, 2013
A publication of AIDIC
The Italian Association of Chemical Engineering
Online at: www.aidic.it/cet
Chief Editors: Sauro Pierucci, Jiří J. Klemeš

ISBN 978-88-95608-23-5; **ISSN** 1974-9791
DOI: 10.3303/CET1332136

Non-linear Analysis of Feedback Controlled Aerobic Cultures

Giuseppe Olivieri[a], Maria Elena Russo[b,*], Erasmo Mancusi[c], Antonio Marzocchella[a,*], Pier Luca Maffettone[a], Piero Salatino[a]

[a] Dipartimento di Ingegneria Chimica, dei Materiali e della Produzione Industriale, Università degli Studi di Napoli Federico II, Piazzale Tecchio 80, 80125, Napoli, Italy
[b] Istituto di Ricerche sulla Combustione – Consiglio Nazionale delle Ricerche, Piazzale Tecchio 80, 80125, Napoli, Italy
[c] Facoltà d'Ingegneria, Università degli Studi del Sannio, Piazza Roma, 21 - I 82100 Benevento, Italy
m.russo@irc.cnr.it

In the present work, the results of a complete dynamical analysis of open- and closed-loop continuous bioreactor for cultures of substrate inhibited aerobic microorganisms were presented. In the closed loop system the dissolved oxygen concentration was controlled at a pre-set value by means of a proportional-integral feedback control scheme manipulating the inlet substrate concentration. A mathematical model was developed coupling the mass balance equation for the substrates (carbon-source and oxygen) and the controller. Solutions of both open- and closed-loop systems were assessed by means of parametric continuation technique and bifurcational analysis tools. The dynamics behavior was studied by changing the main operating parameters – dilution rate and gas-liquid mass transfer rate - and the controller parameters - gain and set-point – in a wide intervals. We have found that the regimes strongly depend on the operating conditions. In particular, the open-loop unstable steady state may be stabilized in closed-loop system, provided the proper choice of both the gain and the reset time for the selected set-point value of oxygen concentration

1. Introduction

Bioreactors operated under continuous steady state conditions are a versatile tool for characterization of microorganism growth kinetics and stoichiometry (Fraleigh et al. 1989; Lodato et al., 2007; Napoli et al., 2011; Napoli et al., 2012; Olivieri et al. 2010; Olivieri et al., 2011). However, the stability of steady state operations of continuous cultures depends on operating conditions (Yano and Koga, 1969; Crooke et al. 1980; Agrawal et al., 1982; Russo et al., 2008). Bioreactor control strategies may stabilize selected regimes and may allow to operate the bioreactor under intrinsically unstable steady states (Edwards, 1970; Edwards et al., 1972). The latter option was also supported by theoretical analyses (Di Biasio et al., 1978; Chang and Chen, 1984; Shimizu and Mastubara, 1985). Auxostat may optimize the bioreactor productivity, avoiding the wash-out conditions (Gostomoski et al., 1994). Turbidostats, nutristats and produstat were successfully proposed in literature (Di Biasio et al., 1981; Agrawal and Lim, 1984, Jayakumar and Lim, 1989; Rutgers et al., 1993; Rutgers et al., 1996; Schröder et al., 1997).
Olivieri et al. (2010) successfully applied the closed-loop oxystat configuration (Hodspoka, 1966) at a continuous bioreactor to stabilize steady state bioconversions. The study was aimed at the assessment of the specific growth rate kinetics of an aerobic *Pseudomonas* strain as a function of phenol, the inhibiting substrate (Viggiani et al., 2006).
The analysis here presented is based on the reconstruction, via parametric continuation, of the solution and the bifurcation diagrams of a mathematical model describing a conventional bioreactor open-loop chemostat and the novel closed-loop oxystat. Both multistability, hysteretic behaviors and periodic regimes are found and described. The inlet substrate concentration, the set point oxygen value and the control gain were adopted as bifurcation parameters. Effects of bifurcation parameters were addressed by means of

Please cite this article as: Olivieri G., Russo M.E., Mancusi E., Marzocchella A., Maffettone P.L., Salatino P., 2013, Non-linear analysis of feedback controlled aerobic cultures, Chemical Engineering Transactions, 32, 811-816 DOI: 10.3303/CET1332136

solution and bifurcation diagrams. A thorough description of static and dynamic attractors was reported for operating and key control parameters typically adopted in experimental investigations.

2. Theoretical framework

The dynamical mathematical model of a continuous stirred tank aerobic bioreactor was characterized by constant dilution rate (D) and the inlet substrate concentration (S^{IN}) in the feeding as manipulated variable. The specific growth rate was characterized by the Haldane-type inhibition model and the Monod-type model as regards the carbon source substrate and oxygen, respectively (Haldane, 1930). The maintenance contributions for substrate and oxygen uptake were included in the stoichiometry of the process (Pirt, 1965). The mass balances - referred to the liquid volume unit - for biomass, substrate, and dissolved oxygen extended to a continuous stirred tank reactor are:

$$\frac{dX}{dt} = -DX + \mu \frac{S}{K_S + S + S^2/K_I} \frac{O_2}{K_{O_2} + O_2} X \tag{1a}$$

$$\frac{dS}{dt} = D\left(S^{IN} - S\right) - \mu \frac{S}{K_S + S + S^2/K_I} \frac{O_2}{K_{O_2} + O_2} \frac{X}{Y_{X/S}} \tag{1b}$$

$$\frac{dS}{dt} = \left(D + K_L a_L\right)\left(S^{IN} - S\right) - \mu \frac{S}{K_S + S + S^2/K_I} \frac{O_2}{K_{O_2} + O_2} \frac{X}{Y_{X/O_2}} \tag{1c}$$

where

$$1/Y_{X/S} = 1/Y^M_{X/S} + m_S/\mu \tag{2a}$$

$$1/Y_{X/O_2} = 1/Y^M_{X/O_2} + m_{O_2}/\mu \tag{2b}$$

The PI feedback control on the state variable O_2 acts as follows:

$$S^{IN}\left(t\right) = S^{IN}_{SS}\left[1 + K_C\left(\frac{O_2^{SET} - O_2}{O_2^{SET}} + 1/T_R \int_0^t \frac{O_2^{SET} - O_2}{O_2^{SET}} dt\right)\right] \tag{3}$$

where O_2^{SET} is the set-point value for O_2, and S^{IN}_{SS} the steady state value of S^{IN} calculated by means of the open-loop system Eq(1a-b-c). The closed-loop system is the combination of Eq(3) in Eq(1a-b-c).
The dimensionless form of model equations was adopted for computation. The following dimensionless variables were introduced:

$$\mathbf{S} = \frac{S}{\sqrt{K_S/K_I}}; \;\; \mathbf{X} = \frac{X}{\sqrt{K_S/K_I}\, Y^M_{X/S}}; \;\; \mathbf{O_2} = \frac{O_2}{O_2^{Eq}}; \;\; \mathbf{t} = t \cdot \mu^M \Big/ \left(2\sqrt{K_S/K_I} + 1\right) \tag{4}$$

Table 1 reports the dimensionless equations describing the closed-loop system.
Bifurcational analysis was carried with the MATCONT tool (Dhooge et al., 2003) of MATLAB® 2010 implementing both the open-loop system and the closed-loop one. The continuation results are presented with two kinds of plots: the solution diagrams for O_2^{SET} and S^{IN} and K_c (bifurcation parameters), and the bifurcation diagram in the plane O_2^{SET}- K_c The solution diagrams report, as a representation of the solution, either the oxygen concentration coming out of the reactor for the steady state solutions, or, for limit cycles, the maximum oxygen concentration value attained during the oscillations. These quantities are plotted versus one of the above indicated bifurcation parameters. The bifurcation diagram illustrates the loci of bifurcation points in the parameter space (Kubíček and Marek, 1983). Some simulation results, for interesting operating situations, are also reported.
The convention adopted for the solution and bifurcation diagrams were: solid lines represent stable stationary solutions; dashed lines unstable stationary solutions; filled circles stable limit cycles; empty circles unstable limit cycles.

3. Results and Discussion

Figure 1A shows the solution diagram as the $\mathbf{S^{IN}}$ is varied for $\mathcal{K}_L$ = 200 and Da = 2. Three solution

Table 1: Dimensionless equation for closed loop system

$\frac{d\mathbf{X}}{d\mathbf{t}} = -\frac{1}{Da}\mathbf{X} + \mu\mathbf{X}$	(T.1.a)
$\frac{d\mathbf{S}}{d\mathbf{t}} = \frac{1}{Da}\left(\mathbf{S}_{SS}^{IN}\left[K_C\left(\frac{\mathbf{O}_2^{SET}-\mathbf{O}_2}{\mathbf{O}_2^{SET}} + \frac{1}{\mathcal{T}_R}\theta\right)+1\right] - \mathbf{S}\right) - (\mu + \mathcal{M}_S)\mathbf{X}$	(T.1.b)
$\frac{d\mathbf{O_2}}{d\mathbf{t}} = \left[\frac{1}{Da} + \mathcal{K}_L\right](1-\mathbf{O}_2) - (\mu + \mathcal{M}_{O2})\mathbf{X}\gamma_{S/O_2}$	(T.1.c)
$\mu = \frac{\mathbf{S}}{\frac{1}{\alpha\beta} + \mathbf{S} + \frac{\alpha}{\beta}\mathbf{S}^2}\frac{\mathbf{O}_2}{\mathcal{K}_{O2} + \mathbf{O}_2}\left(\frac{2+\beta}{\beta}\right)$	(T.1.d)

Table 2: Values of input parameters of the computations.

Model Parameter		*Dimensionless Parameter*	
μ^M	0.26 h^{-1} (1)		
K_S K_I	0.005 g/L (1) 0.20 g/L (1)	$\beta = \sqrt{K_I/K_S}$	6.32
K_{O_2}	10^{-4} g/L (2)	$\mathcal{K}_{O_2} = K_{O_2}/O_2^{Eq}$	0.0128
$Y_{X/S}^M$	1.27 g/g (1)		
Y_{X/O_2}^M	0.17 g/g (2)	$\gamma_{S/O_2} = \left(Y_{X/S}^M\sqrt{K_S K_I}\right)/\left(Y_{X/O_2}^M O_2^{Eq}\right)$	30.3
O_2^{Eq}	$7.8\cdot10^{-3}$ g/L		
m_S	0.017 g/(g h) (1)	$\mathcal{M}_S = m_S Y_{X/S}^M\left(2\sqrt{K_S/K_I}+1\right)/\mu^M$	0.109
m_{O2}	0.040 g/(g h) (1)	$\mathcal{M}_{O_2} = m_{O_2} Y_{X/O_2}^M\left(2\sqrt{K_S/K_I}+1\right)/\mu^M$	0.348
D	0.198-1980 h^{-1}	$Da = \mu^M/\left[D\left(2\sqrt{K_S/K_I}+1\right)\right]$	10^0-10^4
S^{IN}	0.032-3.2 g/L	$\alpha = S^{IN}/\sqrt{K_S K_I}$	10^0-10^2
$K_L a_L$	1.98-1980 h^{-1}	$\mathcal{K}_L = K_L a_L\left(2\sqrt{K_S/K_I}+1\right)/\mu^M$	10^1-10^4
K_C	0.1-10	K_C	0.1-10
T_R	$1.98\cdot10^{-4}$-19.8	$\mathcal{T}_R = T_R\,\mu^M/\left(2\sqrt{K_S/K_I}+1\right)$	10^{-1}-10^1
O_2^{SET}	0-$7.8\cdot10^{-3}$ g/L	$\mathbf{O}_2^{SET} = O_2^{SET}/O_2^{Eq}$	0-1

(1) Olivieri et al. (2010)
(2) Olivieri et al. (2011)

branches exist: 1, 2, and 3. The trivial wash-out solution ($\mathbf{X}^S$=0, $\mathbf{S}^S$=1, $\mathbf{O_2}^S$=1) (3 in Figure1A) exists in all the investigated parameter range. This regime is unstable at low S^{IN} values and become stable after a transcritical bifurcation $TR_{2\text{-}3}$. From the transcritical bifurcation the unstable solution branch (2) emerges. The unstable regimes disappear at $SN_{1\text{-}2}$ as a consequence of a saddle-node bifurcation. It is worth to note that for S^{IN} belong to [$TR_{2\text{-}3}$; $SN_{1\text{-}2}$] three different regimes coexist and only an adequate choice of the initial condition can lead the reactor to operate on the desired ignited regime (1 in Figure1A).

Figure 1B reports the phase portrait $\mathbf{S}^S$ vs. $\mathbf{O_2}^S$ for the steady state 1 and 2 for $\mathcal{K}_L$ = 200 and Da = 2. In comparison with solution 1, the **S** and $\mathbf{O_2}$ values for solution 2 are always larger than 0.2 and a monotonic relationship characterize their relationship.

To elucidate the controller effect time series are reported in Figure 2. The $\mathbf{O_2}$ time series for different value of K_C was reported setting the starting point near the steady solution 1 and the set-point $\mathbf{O_2}^{SET}$ = 0.5. For K_C = 1 the controller was able to approach a steady state condition which corresponds to the solution 2. In this case the stability behavior of solution 1 and 2 was reversed in the closed loop system in comparison with the open-loop system. Indeed, the dynamic of the closed-loop was strongly influenced by the controller parameters. In fact, for K_C = 0.3 no steady solution was approached but a period solution was

observed with large oscillation. Instead, for K_C = 0.1 the system evolution was dramatic: the system approaches the wash-out condition with **X** = 0 and corresponding to the trivial solution 2.
The solution diagrams reported in Figure 3 highlights the effect of K_C (Figure 3A) and of $\mathbf{O_2^{SET}}$ (Figure 3B) on the solution scenario. In both cases the stable regime becomes unstable as a consequence of a dynamical Hopf bifurcation $H_{2\text{-}4}$ and stable periodic regime departs form the Hopf bifurcation point. The continuation schemes allows for the determination of the dynamic branches (4 in Figure 2) emerging from the Hopf bifurcations. The range of existence of the solution 4 was limited by an homoclinic bifurcation (Hom_4) as indicated by the sharp increase of the time period.
A better insight can be obtained by considering the bifurcation diagram in the plane K_C - O_2^{SET} reported in Figures 4 for different $\mathcal{K}_L$ and Da values. The lines reported in this plot divide the parameter space in regions characterized by qualitatively similar phase portraits: Solid lines represent saddle-node bifurcations, dashed lines represent Hopf bifurcations and dotted lines the homoclinic bifurcations. These diagrams allow an easy chose the controller parameters and the operating conditions such that the controller was able to stabilize the steady solution 2. Four regions can be identified:

Region 0) the closed-loop operation is always unsuccessful since there is no solution. According to Figure 2 the set-point $\mathbf{O_2^{SET}}$ is too low with respect to the potential of the reactor.

Region II) the region is characterized by the two steady state solutions 1 (unstable) and 2 (stable).

Region III) the region is characterized by the three solutions: steady-state solutions 1 and 2 and periodic solution 4. The closed-loop operation is not successful because both the steady-state solutions 1 and 2 are unstable. The periodic solution 4 is stabilized by the control action but the oscillation period is quite large: more than five times the characteristic time-scale of the system.

Region IV) No stable solution is present. Steady state solutions 1 and 2 are unstable. The amplitude of the periodic solution 4 increases so much that the periodic solution vanishes through the

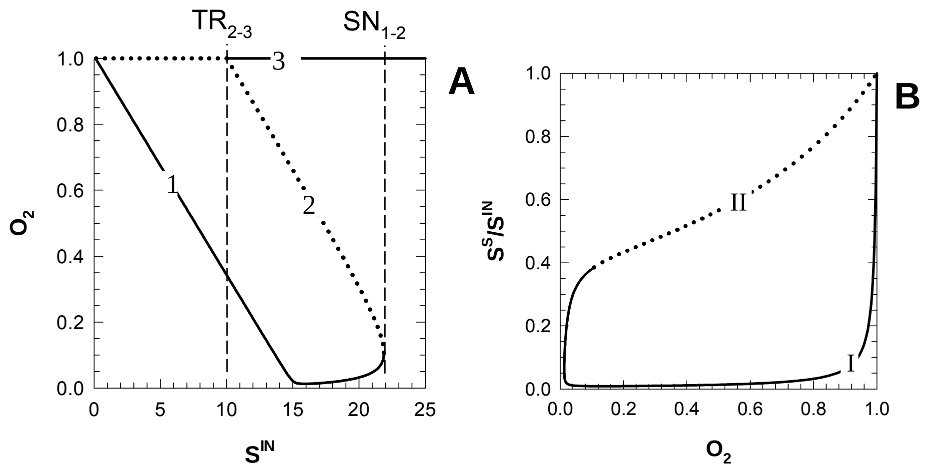

Figure 1: Open-loop system: A) $\mathbf{O_2}$ solution diagram as a function of $\mathbf{S^{IN}}$ for $\mathcal{K}_L$ = 200 and Da = 2; B) Phase portrait $\mathbf{S^S/S^{IN}}$ vs. $\mathbf{O_2^S}$ of steady state solution 1 and 2 for $\mathcal{K}_L$ = 200 and Da = 2.

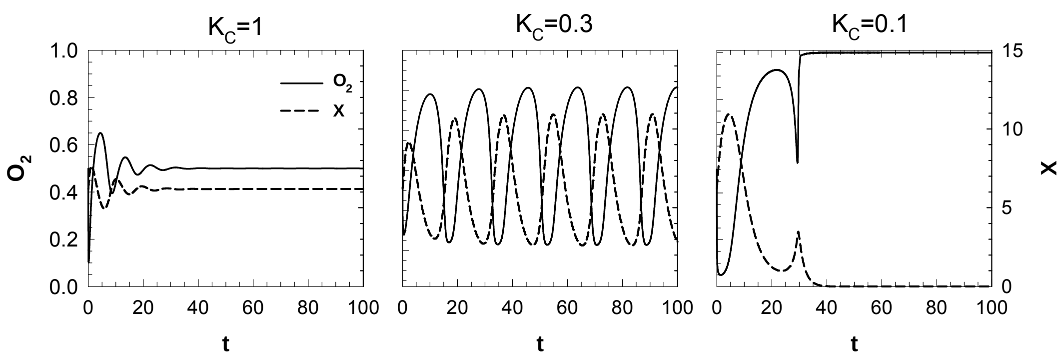

Figure 2: Closed-loop system: $\mathbf{O_2}$ dynamic for different value of K_C. O_2^{SET} = 0.5, $\mathcal{K}_L$ = 200, Da = 2 , $\mathcal{T}_R$ = 1

homoclinic bifurcation Hom_4 with the unstable solution 1. The steady operation under solution 2 is stabilized in the region.

4. Main remarks

The dynamical analysis of a continuous aerobic bioreactor was carried out. The study regarded both a traditional bioreactor and a bioreactor equipped with a controller of the substrate concentration in the feeding stream as a function of the dissolved oxygen concentration. The effects of operating conditions and of controller parameters were characterized. Solution diagrams of state variables as functions of selected continuation parameter were assessed. Results showed that the steady state conditions unstable when operated in the open-loop system - e.g. state characterized by inhibiting level of substrate in the bioreactor - can be stabilized in closed-loop system. The bifurcation analysis suggested that the success of the control asks for an optimal selection of both the gain and the reset time of the controller. In particular, these parameters should be selected in order to avoid oscillating solutions as well as absence of solutions for the continuous operation.

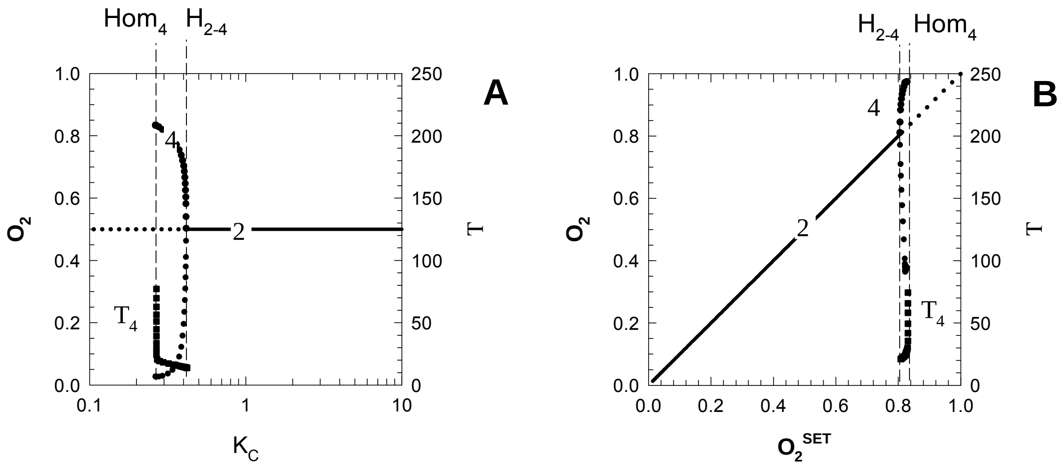

Figure 3: Closed-loop system: A) $\mathbf{O_2}$ solution diagram vs K_C, for $\mathbf{O_2}^{SET}$ = 0.5, $\mathcal{K}_L$ = 200, Da = 2 and $\mathcal{T}_R$ = 1; B) $\mathbf{O_2}$ solution diagram vs $\mathbf{O_2}^{SET}$=0.5 for K_C = 1, $\mathcal{K}_L$ = 200, Da = 2 and $\mathcal{T}_R$ = 1

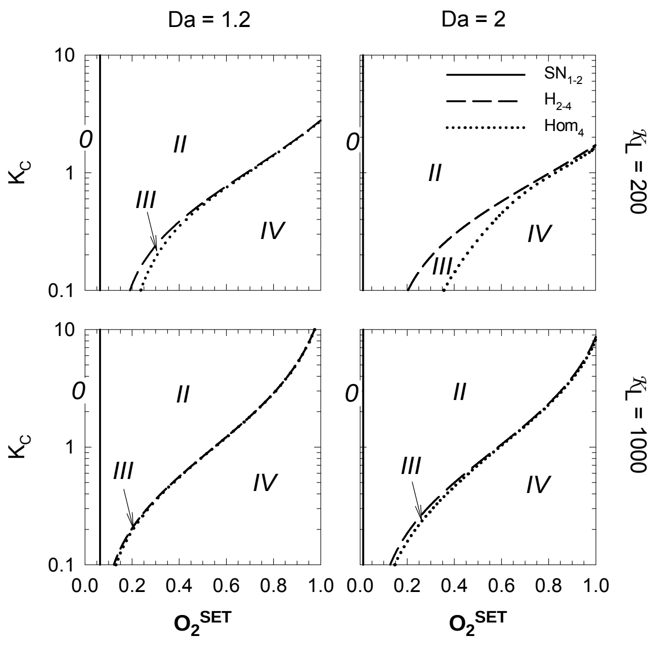

Figure 4: Closed-loop system: K_C vs. O_2^{SET} bifurcation diagrams for $\mathcal{T}_R$ = 1.

References

Agrawal P., Lee C., Lim H.C., Ramkrishna D., 1982, Theoretical investigations of dynamic behaviour of isothermal continuous stirred tank biological reactor, Chem. Eng. Sci. 37, 453-462.

Agrawal T.H., Lim H.C., 1984, Analyses of various control schemes for continuous bioreactors, Adv. Biochem. Eng./Biotechnol. 30, 61-90.

Chang H.C., Chen L.H., 1984, Bifurcation characteristic of nonlinear system under conventional PID control, Chem. Eng. Sci. 7/8, 1127-1142.

Crooke P.S., Wei C.J., Tanner R.D., 1980, The effect of specific growth rate and yield expression on the existence of oscillatory behavior of a continuous fermentation model, Chem. Eng. Comm. 6, 333–342.

Di Biasio D.H., Lim H.C., Weigand W.A., Tsao G.T., 1978, Phase-plane analysis of feedback control of unstable steady states in a biological reactor, AIChE J. 24, 686-693.

Di Basio, D.H., Lim, H.C., Weigand, W.A., 1981, An experimental investigation of stability and multiplicity of steady states in biological reactor, AIChE J., 27, 284–290.

Dhooge A., Govaerts W., Kuznetsov Yu. A., 2003, MATCONT: A MATLAB package for numerical bifurcation analysis of ODEs. ACM Trans Mathem Software, 29, 141-164.

Edwards V.H., 1970, The influence of high substrate concentrations on microbial kinetics, Biotechnol. Bioeng. 12, 679–712.

Edwards V.H., Ko C.R., Balogh A., 1972, Dynamics and control of continuous microbial propagators to subject substrate inhibition, Biotechnol. Bioeng. 14, 939–974.

Fraleigh S.P., Bungay H,R., Clesceri L,S. 1989, Continuous culture, feedback control and auxostats, Trends Biotechnol. 7, 159-164.

Gostomoski P., Mühlemann M., Lin Y.H., Mormino R., Bungay H., 1994, Auxostats for continuous culture research, J. Biotechnol. 37, 167-177.

Haldane J.B.S., 1930, Enzymes. Longmans, London, UK.

Hodspoka J., 1966, Oxygen-absorption rate-controlled feeding of substrate into aerobic microbial cultures. Biotech. Bioeng. 8, 117-134.

Jayakumar S., Lim H.C., 1989, Multiple steady states of *Methylomonas mucosa* for continuous production of polysaccharides, J. Biotechnol. 12, 21-36.

Lodato, A., Alfieri, F., Olivieri, G., Di Donato, A., Marzocchella, A., Salatino, P., 2007, Azo-dye conversion by means of *Pseudomonas* sp. OX1, Enzyme Microb. Technol. 41, 646-652.

Napoli F., Olivieri G., Russo M.E., Marzocchella A., Salatino, P., 2011, Continuous lactose fermentation by *Clostridium acetobutylicum*-Assessment of acidogenesis kinetics, Bioresour. Technol., 102, 1604-1014.

Napoli F., Olivieri G., Russo M.E., Marzocchella A., Salatino P., 2012, Continuous lactose fermentation by *Clostridium acetobutylicum*-Assessment of energetics and product yields of the acidogenesis, Enz. Microb. Technol. 50, 165-172.

Olivieri G., Russo M.E., Di Donato A., Marzocchella A., Salatino P., 2010, Unstable steady state operations of substrate inhibited cultures by dissolved oxygen control, J. Biotechnol. 156, 302-308

Olivieri G., Russo M.E., Marzocchella A., Salatino P., 2011, Modelling of an aerobic biofilm reactor with double-limiting substrate kinetics: bifurcational and dynamical analysis, Biotechnol. Prog. 27, 1599-1613

Pirt S.J., 1965, The maintenance energy of bacteria in growing cultures. Proc. Roy. Soc. B. 163, 224-231.

Russo M.E., Maffettone P.L., Marzocchella A., Salatino P., 2008, Bifurcational and dynamical analysis of a continuous biofilm reactor, J. Biotechnol., 135, 295-303

Rutgers M., Bogte J.J., Breure A.M., Van Andel J.G., 1993, Growth and enrichment of pentachlorophenol-degrading microorganisms in the nutristat, a substrate concentration-controlled continuous culture, Appl. Env. Microbiol. 59, 3373-3377.

Rutgers M., Gooch, D.D., Breure A.M., Van Andel J.G., 1996, Assessment of inhibition kinetics of the growth of strain P5 on pentachlorophenol under steady state conditions in a nutristat, Arch. Microbiol. 165, 194-200

Schröder M., Müller C., Posten C., Deckwer W.D., Hecht V., 1997, Inhibition kinetics of phenol degradation from unstable steady state data, Biotechnol. Bioeng. 54, 567-576.

Shimizu K., Matsubara M., 1985, Conditions for the phase-plane analysis of feedback control of chemostat, Biotech. Bioeng. 27, 519-524.

Viggiani, A., Olivieri, G., Siani, L., Di Donato, A., Marzocchella, A., Salatino, P., Barbieri, P., Galli, E., 2006, An airlift biofilm reactor for the biodegradation of phenol by *Pseudomonas stutzeri* OX1, J. Biotechnol. 123, 464-477.

Yano T., Koga S., 1969, Dynamic behavior of the chemostat subject to substrate inhibition, Biotechnol. Bioeng. 11, 139-153.